Book of Tutorials and Abstracts

European Microbeam Analysis Society

EMAS 2019

16th

EUROPEAN WORKSHOP

on

MODERN DEVELOPMENTS AND APPLICATIONS IN MICROBEAM ANALYSIS

19 to 23 May 2019
at the
NTNU, Realfagbygget
Trondheim, Norway

Organised in collaboration with:
Norwegian University of Science and Technology
(NTNU)

ADVANCES IN ELECTRON CHANNELLING CONTRAST IMAGING AND ELECTRON BACKSCATTER DIFFRACTION FOR IMAGING AND ANALYSIS OF STRUCTURAL DEFECTS IN THE SCANNING ELECTRON MICROSCOPE

Carol Trager-Cowan[1], A. Alasamari[1], W. Avis[1], J. Bruckbauer[1], P.R. Edwards[1], B. Hourahine[1], S. Kraeusel[1], G. Kusch[1], B.M. Jablon[1], R. Johnston[1], R.W. Martin[1], R. McDermott[1], G. Naresh-Kumar[1], M. Nouf-Allehiani[1], E. Pascal[1], D. Thomson[1], S. Vespucci[1], K. Mingard[2], P.J. Parbrook[3], M.D. Smith[3], J. Enslin[4], F. Mehnke[4], M. Kneissl[4,5], C. Kuhn[4], T. Wernicke[4], A. Knauer[5], S. Hagedorn[5], S. Walde[5], M. Weyers[5], P.-M. Coulon[6], P.A. Shields[6], Y. Zhang[7], L. Jiu[7], Y.P. Gong[7], T. Wang[7], O. Navon[8] and A. Winkelmann[1,9]

1 University of Strathclyde, Department of Physics, SUPA
107 Rottenrow East, GlasgowG4 0NG, Great Britain
2 National Physics Laboratory
Teddington TW11 0LW, Great Britain
3 University College Cork, Tyndall National Institute
Cork, Ireland
4 Technische Universität Berlin, Institute of Solid State Physics
10623 Berlin, Germany
5 Leibniz-Institut für Höchstfrequenztechnik, Ferdinand-Braun-Institut
12489 Berlin, Germany
6 University of Bath, Department of Electronic and Electrical Engineering, Centre of Nanoscience and Nanotechnology
Bath BA2 7AY, Great Britain
7 University of Sheffield, Department of Electronic and Electrical Engineering
Sheffield S1 3JD, Great Britain
8 The Hebrew University of Jerusalem, Fredy and Nadine Hermann Institute of Earth Sciences
Jerusalem, Israel
9 Laser Zentrum Hannover eV, Laser Components Department
Hollerithallee 8, 30419 Hannover, Germany
e-mail: nicholas.ritchie@nist.gov

Carol Trager-Cowan graduated with a degree in Natural Philosophy from Glasgow University in 1983, and then went east for a year to St. Andrews University where her MSc-studies found her studying 'hot' electrons in GaAs in the laboratory of Tony Stradling. Her travels then took her south to the laboratory of Doug Heddle at Royal Holloway and Bedford New College, University of London where she spent two and half years constructing, measuring and modelling the properties of electrostatic electron lenses. On completing her PhD in 1987, she returned to Glasgow to work with Brian Henderson and Kevin O'Donnell in the Department of Physics, University of Strathclyde where she studied the luminescence properties of garnets, diamonds and II-VI semiconductors.

In 1990 she was awarded a Fellowship to use electron beams to excite light emission from solids. On April 1st, 1992, she joined the lecturing staff at Strathclyde (promoted to Senior Lecturer in June 1998 and Reader in 2009) and now uses electron beams to interrogate the structure, defects and light emission from solids. Together with her research team and with collaborators from across the world, she works on new developments and novel applications of the scanning electron microscopy techniques of electron backscatter diffraction, electron channelling contrast imaging and cathodoluminescence imaging. In particular, she and her team combine these techniques to, rapidly and non-destructively, analyse defects and their effect on light emission from nitride semiconductors.

1. INTRODUCTION

The scanning electron microscope (SEM) is a very powerful tool for investigating and imaging a wide range of material properties spanning topography, structure, composition and light emission [1-4]. SEM's are extensively used for imaging topography by monitoring the intensity of secondary electrons as a focussed electron beam, with an energy in the range of 100 eV to 30 keV, is rastered over the surface of a sample. Less well known are the techniques of electron channelling contrast imaging (ECCI) [5-12] and electron backscatter diffraction (EBSD) [5-6, 13-14] which exploit diffraction to provide information on crystal structure, crystal misorientation, grain boundaries, strain and structural defects such as dislocations and stacking faults. Here we provide an overview of these techniques and illustrate their application by describing some of our recent investigations of the structural properties of nitride semiconductor thin films and WC-Co hard metals.

2. THE EBSD AND ECCI TECHNIQUES

ECCI and EBSD both exploit diffraction to reveal the structural properties of the crystalline material under investigation. For ECCI it is diffraction of the incident beam, which provides the greatest contrast in the resultant images, while for EBSD it is diffraction of backscattered electrons which provide the crystallographic information. The spatial and depth resolution of these techniques is of the order of tens of nanometres. For successful imaging using either ECCI or EBSD, the sample needs to have a reasonably smooth and clean surface. For the imaging of metal surfaces or the surfaces of geological specimens this usually requires careful sample polishing to produce a high quality surface [10], this is also the case for semiconductor wafers cut from bulk crystals. However, for most epitaxially grown semiconductor thin films no surface preparation is required.

2.1. Electron channelling contrast imaging (ECCI)

ECCI micrographs may be produced when a sample is placed so that a plane or planes are at, or close to, the Bragg angle with respect to the incident electron beam. Any deviation in crystallographic orientation or in lattice constant due to local strain will produce a variation in contrast in the resultant ECCI micrograph. The micrograph is constructed by monitoring the intensity of backscattered or forescattered electrons as the electron beam is scanned over the sample. Extremely small changes in orientation and strain are detectable, revealing, for example, low angle tilt and rotation boundaries and atomic steps. Extended defects such as dislocations and stacking faults may also be imaged [5-12, 15-20].

Figure 1 illustrates the two geometries, namely the backscatter and forescatter geometries, which are used to acquire ECCI micrographs. The backscatter geometry (Fig. 1a) has the advantage that this geometry does not require a high tilt of the sample and therefore a significant correction

of the image to account for tilt is not required. This geometry also allows the easiest imaging of large samples, for example full semiconductor wafers. The forescatter geometry (Fig. 1b) has the advantage that images exhibit better signal-to-noise compared to the backscatter geometry due to the increase in intensity of backscattered electrons. The detector used to detect the backscattered electrons is generally an electron-sensitive diode. Key to the acquisition of good quality ECCI micrographs is the use of a good amplification system.

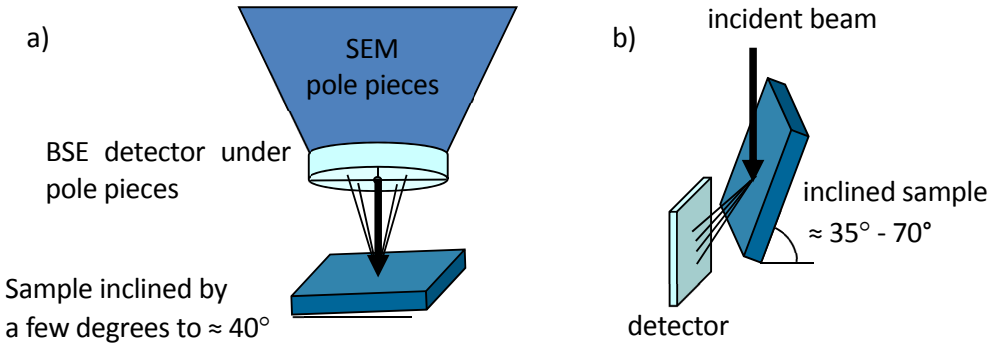

Figure 1. Illustrating the a) backscatter and b) forescatter geometries for acquisition of ECCI micrographs.

2.2. Electron backscatter diffraction (EBSD

In EBSD the sample is tilted at around 70° to the normal of the incident SEM beam. The impinging electrons are scattered inelastically through high angles forming a diverging source of electrons, which can be diffracted. The resultant electron backscatter diffraction pattern (EBSP) consists of a large number of overlapping bands, known as Kikuchi bands, which are closely related to a 2D projection of the crystal structure, where each Kikuchi band corresponds to a set of planes, as illustrated in Fig. 2b. The EBSP is generally detected by an electron sensitive phosphor or scintillator screen and a CCD or CMOS camera [13] (see Fig. 2a), although there have been recent developments of direct electron cameras [21-22]. The EBSP shown in Fig. 2b was acquired at 20 keV from a Si sample using energy-filtered direct electron detection with a collection angle of ≈ 50°. Direct electron detection allows high quality EBSPs to be acquired at low electron beam energies, pattern acquisition down to 3 keV is achievable [22]. EBSD is a well-established technique for texture analysis and for quantifying grain boundaries and crystal phases [5-6, 13-14]. The introduction of cross-correlation based analysis of EBSPs has also made possible measurements of relative strain, geometrically necessary dislocations, and lattice tilt and twist [14, 23], antiphase domains [24] and crystal polarity [25].

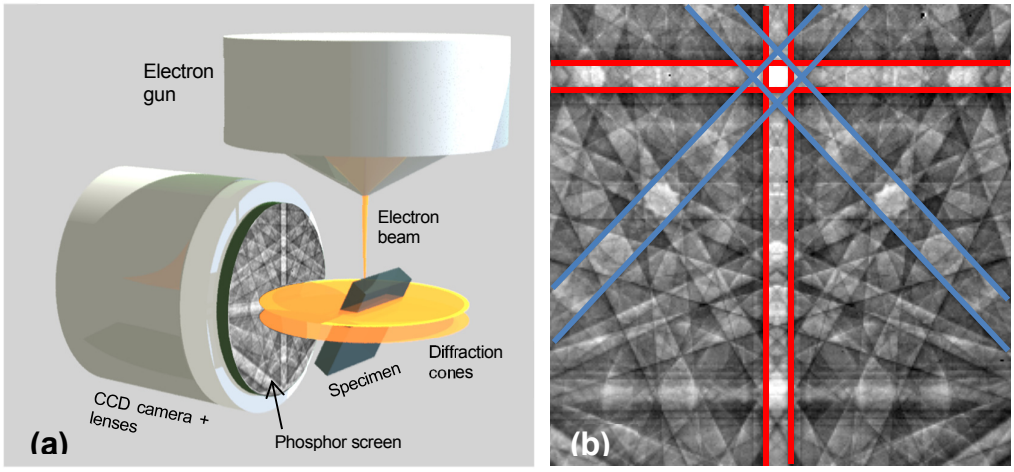

Figure 2. a) Illustration of the EBSD detection geometry and a conventional EBSD detector. b) An EBSP from Si acquired at an energy of 20 keV with a collection angle of ≈ 50°. The red lines outline Kikuchi bands corresponding to {200} planes, the blue lines outline Kikuchi bands corresponding to {220} planes. Adapted from [22] under Creative Commons Attribution (CC BY) license: http://creativecommons.org/licenses/by/4.0/.

3. *EXAMPLE RESULTS*

3.1. *The use of ECCI to image sub-grains and dislocations in a GaN thin film*

Figure 3a shows an ECCI micrograph of a GaN thin film grown on c-plane sapphire by metalorganic vapour phase epitaxy (MOVPE). T he ECCI micrograph was acquired at an electron beam energy of 30 keV in the forescatter geometry in an FEI Sirion 200 Schottky field emission gun SEM (Sirion SEM). The variation in grey scale in the ECCI micrograph is a result of small differences in orientation of sub-grains in the thin film. This is highlighted in the pseudo-colour image of Fig. 3b. The "spots" in the image, most of which exhibit a black-white contrast (see inset of Fig. 3a for example), are threading dislocations; that is dislocations which thread through the thin film and are caused by the growth on the lattice-mismatched sapphire substrate. The threading dislocations propagate to the surface of the sample and are revealed due to associated strain fields [26]. A large number of the threading dislocations are seen to lie on sub-grain boundaries. Note that in order to reveal all misorientations, and thus all the sub-grain boundaries, a number of ECCI micrographs need to be acquired under a range of diffraction conditions [27]. To select a particular diffraction condition, that is accurately select the plane or planes to diffract the incident beam (usually referred to as selecting the **g**-vector), it is necessary to acquire an electron channelling pattern (ECP). This is discussed in Section 3.2. While the contrast in the ECCI micrograph reveals the presence of sub-grains, it does not provide any quantitative information on their orientation. The magnitude and direction of misorientation can be measured by EBSD, and an EBSD study of sub-grain orientations for an AlN thin film is presented in Section 3.3.

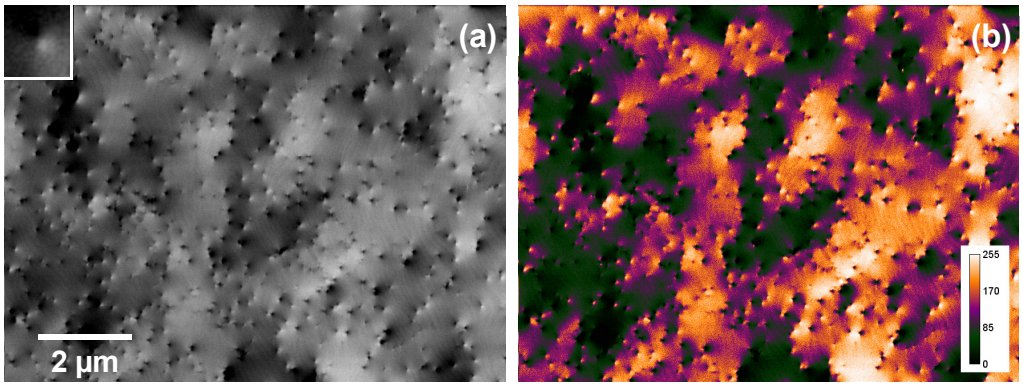

Figure 3. ECCI micrograph from a GaN thin film presented as a) a grey scale image, and b) a pseudo-colour image.

3.2. Selection/determination of the diffraction condition for ECCI, acquiring ECPs

An ECP is obtained when changes in the backscattered electron intensity are recorded as the angle of the incident electron beam is changed relative to the surface of a single crystal area of the sample. When the beam changes its angle with respect to the sample, different planes of the crystal satisfy the Bragg condition, giving rise to the appearance of overlapping Kikuchi bands superimposed on the image of the sample; an ECP from a GaN thin film is shown in Fig. 4. The ECP, like an EBSP (the two are related by reciprocity), is closely related to the 2D projection of the crystal structure, with the Kikuchi bands corresponding to different planes in the crystal. Comparing the ECP with kinematical and/or dynamical electron diffraction simulations allows the pattern to be indexed: i.e., the planes in the ECP can be identified. The plane (or planes) which intersect the centre of the ECP, usually referred to as the pattern centre (PC), are those from which the incident electron beam is diffracted. In the example shown in Fig. 4, the incident electron beam was diffracted from one of the {11 20} planes; that is a **g**-vector of <11 20> was selected.

An ECP may be obtained by acquiring a backscattered image at low magnification. At low magnification, as the beam is scanned over the sample, it changes its angle with respect to the surface of the sample (in our case, for our Sirion SEM, this is by around ± 2.5°), allowing an ECP to be obtained [11]. Note that this method of acquiring an ECP is only possible if the scanned area of the sample (of order 5 mm × 5 mm in size) is smooth and all of the same crystallographic orientation. An ECCI micrograph is obtained on zooming in on the PC by increasing the magnification. At higher magnification the beam has a fixed angle with respect to the sample surface as the beam is scanned. The resultant ECCI micrograph will reveal any defects, which distort the plane or planes which correspond to the Kikuchi bands intersecting the PC. Alternatively, if 'beam rocking' electron optics are available in the SEM, the angle of the beam with respect to the sample can be changed over a much smaller surface area. Selected area ECPs, referred to as SAECPS or SACPs can be acquired from areas ranging from a

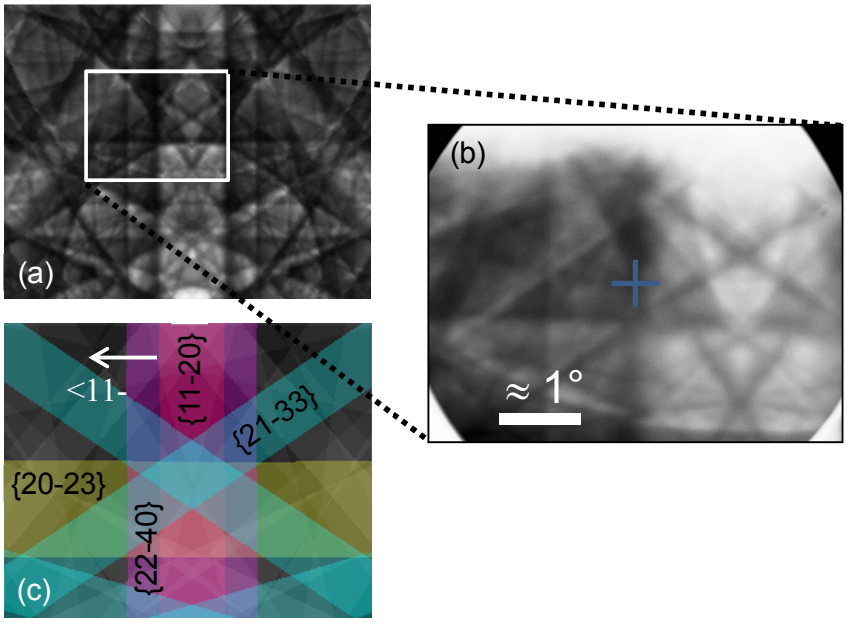

Figure 4. a) Dynamical simulation of an electron channelling pattern (ECP) from a GaN thin film. Electron beam energy is 30 keV, sample tilt ≈ 40°. b) Experimental ECP. The blue cross marks the pattern centre (PC). c) Kinematical simulation of the ECP with some indexed planes highlighted (produced with ESPRIT DynamicS (Bruker Nano) software). In this case the PC intersects with the edge one of the {11-20} Kikuchi bands, so a **g**-vector of <11-20> was selected.

10 µm × 10 µm down to of order 500 nm × 500 nm in size [28]. While a lot of useful information can be obtained from ECCI without the acquisition of ECPs, the ability to acquire ECPs makes ECCI far more powerful and easier to use, in particular when it is applied to the identification of unknown extended defects such as dislocations and stacking faults.

3.3. The use of ECCI and EBSD to investigate sub-grains and dislocations in an AlN thin film

Figure 5 shows ECCI micrographs and EBSD maps from an AlN thin film overgrown by MOVPE on a nanopatterned sapphire substrate (nPSS). In this case the experiments were performed in a FEI Quanta 250 Schottky field emission gun environmental/variable pressure SEM (Quanta SEM) equipped with an Oxford Instruments Nordlys EBSD detector and forescatter diodes for EBSD and ECCI measurements respectively where the SEM was operated in low vacuum mode (0.5 mbar) to avoid charging of this insulating specimen.

The contrast in the ECCI micrograph of Fig. 5a is a result of small differences in orientation of sub-grains in the thin film. The inset shows a higher resolution ECCI micrograph where threading dislocations propagating to the surface of the sample are revealed. A significant number of the TDs are located on the sub-grain boundaries. As stated previously in Section 3.1, while ECCI reveals differences in orientation between sub-grains, it does not provide a measure

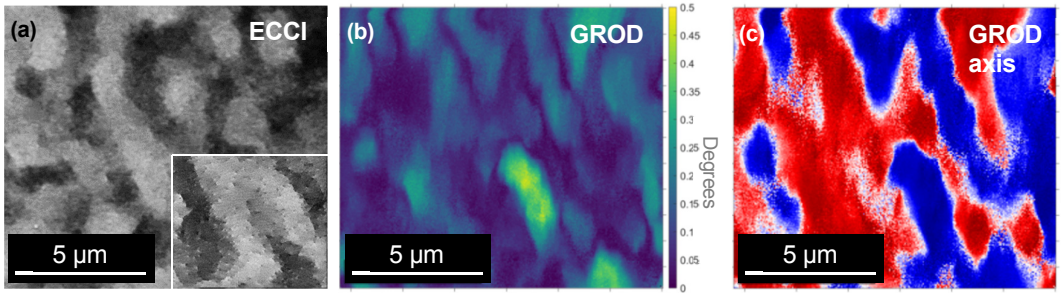

Figure 5. ECCI micrographs and EBSD maps from an AlN thin film. a) ECCI micrograph, acquired at an electron beam energy of 25 keV, revealing sub-grains. The inset shows a higher resolution ECCI micrograph revealing threading dislocations ("spots" exhibiting black-white contrast). b) grain reference orientation deviation (GROD) map, and c) and grain reference orientation deviation axis (GROD axis) map where the colours denote direction of in-plane rotation (i.e., around the c-axis). The red regions are rotated in the opposite direction to the blue regions. The GROD and GROD axis maps were derived from EBSD data acquired at 20 keV. Note that the ECCI micrograph and EBSD maps were acquired from the same sample, but not from the same area of the sample.

of the magnitudes and directions of these misorientations. Figure 5b shows a grain reference orientation deviation (GROD) map (the deviation of orientation of the sub-grains relative to an average orientation [29]) derived from EBSD data using MTEX [30]. In this case, the first step of the analysis involved comparison of each EBSP with dynamical simulations [31]. Figure 5c is a GROD axis map which reveals that the sub-grains are rotated relative to each other, where the rotation axis is out of plane, i.e., around the c-axis, often referred to as twist. The colours, blue and red, denote the direction of in-plane rotation. The red regions are rotated in the opposite direction to the blue regions.

The results presented above illustrate how ECCI and EBSD can provide complementary structural information. ECCI allows fast determination of dislocation densities and their distribution and reveals the presence of sub-grains, Fig. 5 and its inset each took around 10 minutes of direct acquisition. EBSD provides quantitative information on the magnitude and direction of the misorientations in the film. However the EBSD data from which the maps of Fig. 5 were derived, took of order three hours to acquire. The EBSD data acquisition was then followed by further data analysis which is also time-consuming. In spite of this, both techniques share the advantages of being non-destructive and can be used to interrogate large areas of a sample.

3.4. The use of ECCI and EBSD to investigate sub-grains in an as-sintered WC-Co hard metal sample

Figure 6 shows a) an ECCI micrograph, b) a GROD map, and c) a GROD axis map from WC-grains of an as-sintered WC-Co hard metal sample. The ECCI micrograph and EBSD maps reveal sub-grains within nominally single crystal WC-grains, indicating how the large grains

may have evolved during the sintering process. ECCI also reveals dislocations and stacking faults within the WC-grains [32]. In this case the EBSD derived maps again provide quantification of the sub-grain misorientations. In this case, the GROD axis map reveals the misorientations are around more than one axis. The colour key indicates the direction of the misorientation axes in real space above (upper hemisphere) or below (lower hemisphere) the sample. The black dots indicate these directions for each point in the map.

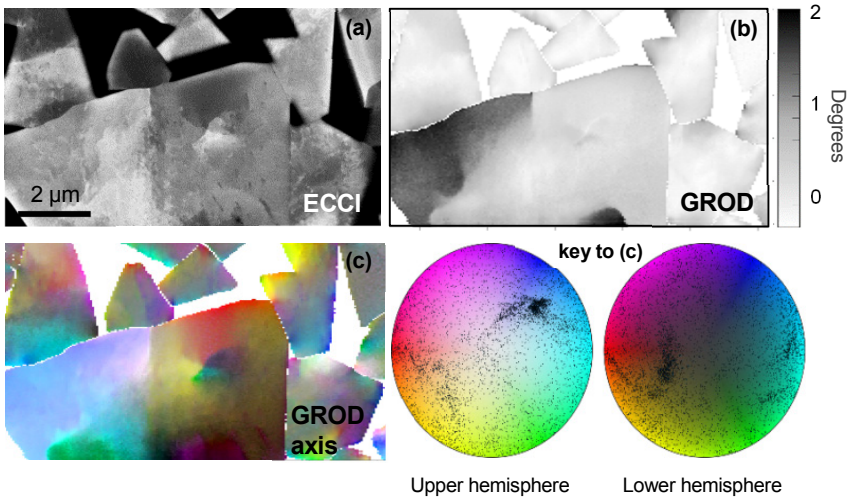

Figure 6. ECCI and EBSD maps from WC-grains of an as-sintered WC-Co hard metal. a) ECCI micrograph acquired at 20 keV, b) GROD map, and c) a GROD axis map. The GROD and GROD axis maps were derived from EBSD data acquired at 20 keV. Note in this case the ECCI micrograph and EBSD maps were acquired from the same area of the sample.

4. *SUMMARY*

To summarise we have shown that ECCI allows direct, fast imaging of dislocations and sub-grain boundaries, while EBSD provides quantitative information on the magnitude and direction of misorientations a sample. Both techniques share the advantages of being non-destructive and can be used to interrogate and provide valuable information on defects from large areas of a sample.

5. *REFERENCES*

[1] Holt D B and Joy D C 1989 *SEM microcharacterization of semiconductors*. (New York, NY: Academic Press

[2] Goldstein J, Newbury D, Joy D, Lyman C, Echlin P, Lifshin E, Sawyer L and Michael J 2007 *Scanning electron microscopy and X-ray microanalysis*. (New York, NY: Springer)

[3] Reimer L 1998 *Scanning electron microscopy: Physics of image formation and microanalysis*. (New York, NY: Springer)
[4] Zhou W and Wang Z L 2007 *Scanning microscopy for nanotechnology: techniques and applications*. (New York, NY: Springer Science & Business Media)
[5] Wilkinson A J and Hirsch P B 1997 Electron diffraction based techniques in scanning electron microscopy of bulk materials. *Micron* **28** 279-308
[6] Trager-Cowan C, Sweeney F, Trimby P W, Day A P, Gholinia A, Schmidt N H, Parbrook P J, Wilkinson A J and Watson I M 2007 Electron backscatter diffraction and electron channeling contrast imaging of tilt and dislocations in nitride thin films. *Phys. Rev. B* **75** 085301
[7] Crimp M A, Simkin B A and Ng B C 2001 Demonstration of the g·bxu=0 edge dislocation invisibility criterion for electron channelling contrast imaging. *Philos. Mag. Lett.* **81** 833-837
[8] Picard Y, Kamaladasa R, De Graef M, Nuhfer N, Mershon W, Owens T, Sedlacek L and Lopour F 2012 Future Prospects for Defect and Strain Analysis in the SEM via Electron Channeling. *Microsc. Today* **20**(2) 12-16
[9] Naresh-Kumar G, Hourahine B, Edwards P R, Day A P, Winkelmann A, Wilkinson A J, Parbrook P J, England G and Trager-Cowan C 2012 Rapid nondestructive analysis of threading dislocations in wurtzite materials using the scanning electron microscope. *Phys. Rev. Lett.* **108** 135503
[10] Zaefferer S and Elhami N N 2014 Theory and application of electron channelling contrast imaging under controlled diffraction conditions. *Acta Mater.* **75** 20-50
[11] Deitz J I, Carnevale S D, Ringel S A, McComb D W and Grassman T J 2015 Electron Channeling Contrast Imaging for Rapid III-V Heteroepitaxial Characterization. *J. Vis. Exp.* **101** e52745
[12] Naresh-Kumar G, Thomson D, Nouf-Allehiani M, Bruckbauer J, Edwards P R, Hourahine B, Martin R W and Trager-Cowan C 2016 Electron channelling contrast imaging for III-nitride thin film structures. *Mater. Sci. Semicond. Process.* **47** 44-50
[13] Schwartz A J, Kumar M, Adams B L and Field D P 2009 *Electron backscatter diffraction in materials science*. (New York, NY: Springer)
[14] Wilkinson A J and Britton T B 2012 Strains, planes, and EBSD in materials science. *Mater. Today* **15**(9) 366-376
[15] Naresh-Kumar G, Mauder C, Wang K R, Kraeusel S, Bruckbauer J, Edwards P R, Hourahine B, Kalisch H, Vescan A, Giesen C and Heuken M 2013 Electron channeling contrast imaging studies of nonpolar nitrides using a scanning electron microscope. *Appl. Phys. Lett.* **102** 142103
[16] Carnevale S D, Deitz J I, Carlin J A, Picard Y N, De Graef M, Ringel S A and Grassman T J 2014 Rapid misfit dislocation characterization in heteroepitaxial III-V/Si thin films by electron channeling contrast imaging. *Appl. Phys. Lett.* **104** 232111
[17] Hite J K, Mastro M A and Eddy Jr C R 2010 Approach for dislocation free GaN epitaxy. *J. Cryst. Growth* **312** 3143-3146

[18] Schulze A, Strakos L, Vystavel T, Loo R, Pacco A, Collaert N, Vandervorst W and Caymax M 2018 Non-destructive characterization of extended crystalline defects in confined semiconductor device structures. *Nanoscale* **10** 7058-7066

[19] Callahan P G, Haidet B B, Jung D, Seward G G and Mukherjee K 2018 Direct observation of recombination-enhanced dislocation glide in heteroepitaxial GaAs on silicon. *Phys. Rev. Mater.* **2** 081601

[20] Yaung K N, Kirnstoetter S, Faucher J, Gerger A, Lochtefeld A, Barnett A and Minjoo L L 2016 Threading dislocation density characterization in III–V photovoltaic materials by electron channeling contrast imaging. *J. Cryst. Growth* **453** 65-70

[21] Wilkinson A J, Moldovan G, Britton T B, Bewick A, Clough R and Kirkland A I 2013 Direct detection of electron backscatter diffraction patterns. *Phys. Rev. Lett.* **111** 065506

[22] Vespucci S, Winkelmann A, Naresh-Kumar G, Mingard K P, Maneuski D, Edwards P R, Day A P, O'Shea V and Trager-Cowan C 2015 Digital direct electron imaging of energy-filtered electron backscatter diffraction patterns. *Phys. Rev. B* **92** 205301

[23] Wilkinson A J, Meaden G and Dingley D J 2006 High-resolution elastic strain measurement from electron backscatter diffraction patterns: new levels of sensitivity. *Ultramicroscopy* **106** 307-313

[24] Naresh-Kumar G, Vilalta-Clemente A, Jussila H, Winkelmann A, Nolze G, Vespucci S, Nagarajan S, Wilkinson A J and Trager-Cowan C 2017 Quantitative imaging of anti-phase domains by polarity sensitive orientation mapping using electron backscatter diffraction. *Scientif. Rep.* **7** 10916

[25] Winkelmann A, Nolze G, Himmerlich M, Lebedev V and Reichmann A 2016 Point-Group Sensitive Orientation Mapping Using EBSD. in: *Proc. 6th Int. Conference on Recrystallization and Grain Growth*. (Holm E A, Farjami S, Manohar P, Rohrer G, Rollett A D, Srolovitz D and Weiland H; Eds.) (New York, NY: Springer) 281-286

[26] Pascal E, Hourahine B, Naresh-Kumar G, Mingard K and Trager-Cowan C 2018 Dislocation contrast in electron channelling contrast images as projections of strain-like components. *Mater. Today: Proc.* **5** 14652-14661

[27] Day A P and Quested T E 1999 A comparison of grain imaging and measurement using horizontal orientation and colour orientation contrast imaging, electron backscatter pattern and optical methods. *J. Microscopy* **195** 186-196

[28] Mansour H, Guyon J, Crimp M A, Gey N, Beausir B and Maloufi A N 2014 Accurate electron channeling contrast analysis of dislocations in fine grained bulk materials. *Scripta Mater.* **84** 11-14

[29] Wright S I, Nowell M M and Field D P 2011 A review of strain analysis using electron backscatter diffraction. *Microsc. Microanal.* **17** 316-329

[30] Bachmann F, Hielscher R and Schaeben H 2010 Texture analysis with MTEX - Free and open source software toolbox. *Solid State Phenomena* **160** 63-68

[31] Winkelmann A, Trager-Cowan C, Sweeney F, Day A P and Parbrook P J 2007 Many-beam dynamical simulation of electron backscatter diffraction patterns. *Ultramicroscopy* **107** 414-421

[32] Jablon B M, *et al.* 2019 in preparation